## CASIM

A. Van Ginneken developed this program (Va75). It was designed to simulate the average behavior of hadrons in the region 10 to 1000 GeV and has been extended to 20 TeV (Va87). It uses inclusive production distributions directly in order to obtain the particles to follow. The particle production algorithm is based upon the Hagedorn-Ranft thermodynamic model. Only one or two high energy particles are created in each collision and these carry a weight related to the probability of their production and the energy carried with them. Path length stretching and particle splitting have been introduced. Electromagnetic showers resulting from $\pi^o$ production are calculated using the companion code AEGIS. Simple "standardized" geometries are available. However, the user generally writes a FORTRAN subroutine to set up the geometry of interest. This subroutine consists of "logical" (i.e., "IF", etc.) statements used to deduce the material or magnetic field in which a particle being tracked is found at a given "time" in the calculation from the particle's spatial and directional coordinates. The program readily allows magnetic fields to be used. A muon version called CASIMU (now MUSIM) has been written (Va87). The accuracy of the hadron version has been verified for energies up to 800 GeV (Co82a and Co85a). The muon version has also been verified for energies up to 800 GeV for production and transport of muons in real-life, complicated shields (Co89a and Co89b). Normally, CASIM is not set up to follow particles with momenta less than 300 MeV/c, which corresponds to a kinetic energy of 47 MeV for nucleons. All low energy phenomena, then, is obtained by matching energy spectra and fluence at this energy with results of codes capable of tracking lower energy particles (e.g., HETC, FLUKA, and MARS). At Fermilab, CASIM has largely been replaced by MARS as the code of choice.

## EGS

EGS, electron gamma shower code is a powerful code for calculating electromagnetic cascades. The most recent version is EGS4. A complete description of this code system has been written by Nelson et al. (Ne85, Ne90). This program provides a Monte Carlo analysis of electron and photon scattering including shower generation. The lower limit of its validity is about 10 keV while the upper limit of its validity is at least 1 TeV. Possible target materials span the periodic table. As the electron encounters target atoms, it is scattered randomly to mimic the known mechanisms of electron scattering. When secondary particles arise, they are loaded into a stack from which EGS4 selects sequentially the lowest energy particle and then traces out its further path until it leaves the target or until its energy falls below a selected cut-off value. The final kinematical and charge properties of all the particles are noted and summed for all particles in the shower concluding with a "history" of all of them. Improvements with the code are continuously being made. The code is a cornerstone at many laboratories that have electron accelerators. The code has been found to be extremely useful in applications in medicine and also in modeling the performance of high energy physics apparatus. The EGS code system is available from the Stanford Linear Accelerator Center (present URL: http://www.slac.stanford.edu/cgi-bin/spiface/find/freehep/www?name=EGS4.)

## FLUKA

FLUKA is an integrated, versatile multi-particle Monte Carlo program, capable of handling a wide variety of radiation transport problems. Its energy range extends from one keV (for neutrons, thermal energies) to thousands of TeV. FLUKA can simulate with a similar level of accuracy the propagation of hadronic and electromagnetic cascades, cosmic muons, slowing-down neutrons and synchrotron radiation in the keV region. An original treatment of multiple Coulomb scattering allows the code to handle accurately some challenging problems such as electron backscattering and energy deposition in thin layers. In a fully analog mode, FLUKA can be used in detector studies to predict fluctuations, coincidences and anti-coincidences. On the other hand, a rich supply of biasing options makes it well suited for studies of rare events, deep penetration and shielding in general. This code originated as high-energy particle transport code developed by a CERN-Helsinki-Leipzig collaboration, principally by J. Ranft as discussed by Aarnio, et al. (Aa86). More recently, it has been completely rewritten and extended to low energies as discussed by Fassò et al. (Fa93). It handles more than 30 different particles, including neutrons from thermal energies to about 20 TeV and photons from 1 keV to thousands of TeV. Several biasing techniques are available. Recoil protons and protons from N(n,p) reaction are transported explicitly. This code is currently available from the Stanford Linear Accelerator Center (present URL: http://www.slac.stanford.edu/esh/rp/assign.html.)

## HETC and LAHET

This code, developed over many years under the leadership of R. G. Alsmiller at the Oak Ridge National Laboratory, is considered by some to be the benchmark hadron shielding code of choice. It has been upgraded many times and can, in suitably augmented versions, follow particles from the 20 TeV region down to thermal energies. It is an extremely flexible code but has the important disadvantage that the individual events are written to mass storage. It is the responsibility of the user to write a program to analyze the results. In terms of CPU-time HETC is also relatively slow so that calculations to be done should be carefully selected. It is seen to be preferable to use selected HETC runs to calibrate another faster, but less accurate code. It has been described by Armstrong (Ar80) and Gabriel (Ga85). It now uses the same event generator used for FLUKA. A modified version of this code, developed at the Los Alamos National Laboratory (LANL) as LAHET, has been described by Prael and Lichtenstein (Pr89). It is available from the LANL (present URL: http://www-xdiv.lanl.gov/XCI/PROJECTS/LCS/). This variant permits the transport of neutrons, photons, and light nuclei up to $^4$He and employs the geometric capabilities of the MCNP code.

## MARS

The MARS Monte Carlo code system has been developed over a number of years by N. Mokhov, et al. (Ka89, Mo95, and Kr97). Results using early versions of this code were compared by Mokhov and Cossairt (Mo86) with those obtained using then-current versions of CASIM and FLUKA. Good agreement was obtained in this study. The code allows fast inclusive simulation of three-dimensional hadronic and electromagnetic cascades for shielding, accelerator, and detector components in the energy range from a fraction of an electronvolt up to 100 TeV. The current version uses the phenomenological model for inclusive hadron- and photon-nucleus interactions for $E > 5$ GeV and exclusive cascade-exciton model at 1 MeV $< E <$ 5 GeV. It includes photo- and electro-production of hadrons and muons, improved algorithms for the 3-body decays, precise particle tracking in magnetic fields, synchrotron radiation by electrons and muons, significantly extended histogramming capabilities and material description, improved computational performance. In addition to the direct energy deposition calculations, a set of dose conversion per fluence factors for all particles including neutrinos is built into the code. The code includes links to the MCNP4A code for neutron and photon transport below 20 MeV, to the ANSYS code for thermal and stress analyses and to the code for multi-turn particle tracking in large synchrotrons and collider rings. The geometry module allows a set of the pre-defined shapes, arbitrary user-defined 3-D description, or uses the object-oriented engine coupled with VRML/2.0 - the newly approved standard for a 3-D World Wide Web-oriented geometry description. This allows one to rely on a convenient VRML-enabled WWW browser for a navigation through the entire geometry, a link of the geometry description to the user Web page and a visualization of the output results with a possible scripting. The geometry module is linked to the object-oriented database for a fast storage/retrieving of complex geometries. The developments were induced by numerous challenging applications - Fermilab accelerator, detector and shielding upgrades, Large Hadron Collider machine and detector studies, muon colliders etc - as well as by a continuous desire to increase code reliability, flexibility and user friendliness. This code is available from Fermilab (present URL: http://www-ap.fnal.gov/MARS/)

## MCNP

MCNP is a general-purpose Monte Carlo N-particle code that can be used for neutron, photon, electron, or coupled neutron/photon/electron transport, including the capability to handle situations involving nuclear criticality. This code has been developed at the Los Alamos National Laboratory and is well documented in LANL reports (e.g., Br97). It is available through Oak Ridge National Laboratory’s Radiation Shielding Information Computation Center (RSICC). The code treats an arbitrary three-dimensional configuration of materials in geometric cells bounded by first- and second-degree surfaces and fourth-degree elliptical tori. The neutron energy regime is from $10^{-11}$ MeV to 150 MeV, and the photon and electron energy regimes are from 1 keV to 1000 MeV. For neutrons, all reactions given in a particular cross-section evaluation (such as ENDF/B-VI cross section database) are accounted for. Thermal neutrons are described by both the free gas and thermal particle scattering models. For photons, the code takes account of incoherent and coherent scattering, the possibility of fluorescent emission after photoelectric absorption, absorption in pair production with local emission of annihilation radiation, and bremsstrahlung. A continuous slowing down model is used for electron transport that includes positrons, k x-rays, and bremsstrahlung but does not include external or self-induced fields. Important standard features that make MCNP very versatile and easy to use include a powerful general source, criticality source, and surface source; both geometry and output tally plotters; a rich collection of variance reduction techniques; a flexible tally structure (including a pulse-height tally); and an extensive collection of cross-section data. The present URL is http://www-xdiv.lanl.gov/x5/MCNP/index.html.

As was discussed in Section 4.7.2, a convenient way to exhibit the "raw" output of Monte Carlo high energy hadronic cascade calculations is in the form of contour plots of star density as a function of longitudinal coordinate, *Z*, and radial coordinate, *R*. This appendix contains representative samples of such plots. This collection is not intended to address all situations and the main text refers to more complete compilations of calculations. Individual calculations should be done for definitive results.

The examples provided here are of three general classes:

Figures B1.a-B1.d are for protons incident along the axis of a solid CONCRETE cylinder perpendicular to one face of the cylinder. The concrete is of "standard" composition" and is taken to have a density of 2.4 g $cm^{-3}$.

Figures B2.a-B2.d are for protons incident along the axis of a solid IRON cylinder perpendicular to one face of the cylinder. The iron is taken to have a density of 7.87 g $cm^{-3}$.

Figures B3.a-B3.d are for 1 TeV protons incident on various beamline components that might be found in a typical beam enclosure consisting of a cylindrical tunnel with CONCRETE walls surrounded by a concentric cylindrical SOIL shield. For the components, the standard densities found in Table 1.2 were used. The density of concrete was taken to be 2.4 g $cm^{-3}$ and the density of soil was taken to be 2.25 g $cm^{-3}$. Beam pipes were assumed taken to be at vacuum. The captions describe the details of the beam loss scenarios used in the calculations.

## B.1 Results for Solid CONCRETE Cylinders

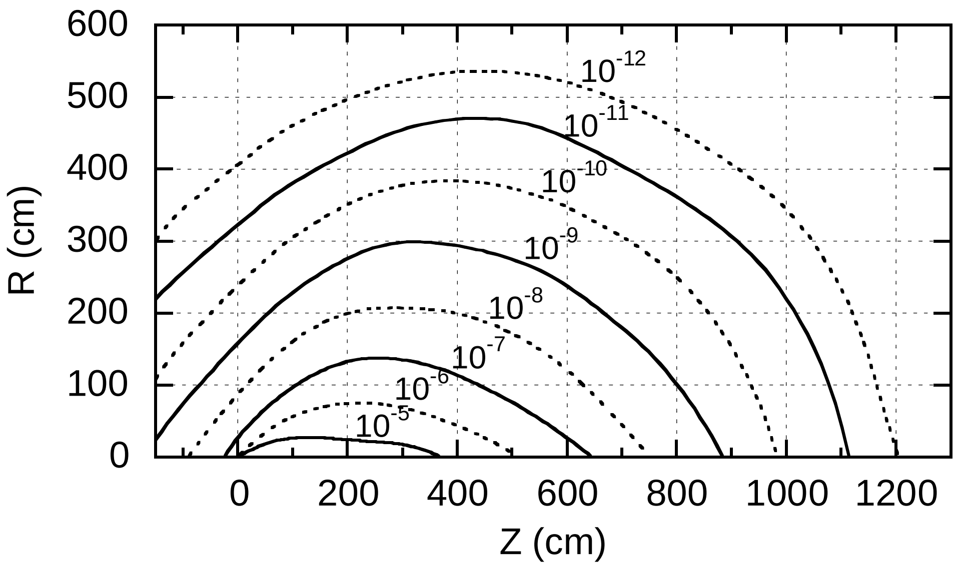


Fig. B1.a Monte Carlo results for 30 GeV/c protons incident on a CONCRETE cylinder. Contours of equal star density (stars cm$^{-3}$) per incident proton are plotted. The beam of 0.3 x 0.3 cm cross section is centered on the cylinder axis and starts to interact at zero depth. The star density includes only those due to hadrons above 0.3 GeV/c momentum. Contours of higher star density are not shown for clarity while those of lower star density are not included due to statistical uncertainty. [Adapted from (Va75).]

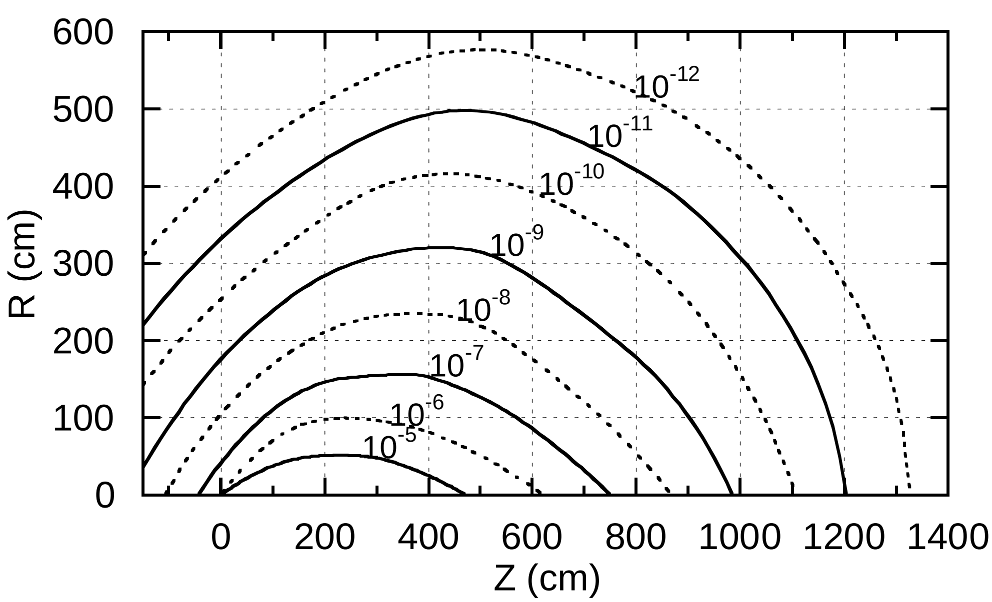


Fig. B1.b Monte Carlo results for 100 GeV/c protons incident on a CONCRETE cylinder. Contours of equal star density (stars cm$^{-3}$) per incident proton are plotted. The beam of 0.3 x 0.3 cm cross section is centered on the cylinder axis and starts to interact at zero depth. The star density includes only those due to hadrons above 0.3 GeV/c momentum. Contours of higher star density are not shown for clarity while those of lower star density are not included due to statistical uncertainty. [Adapted from (Va75).]

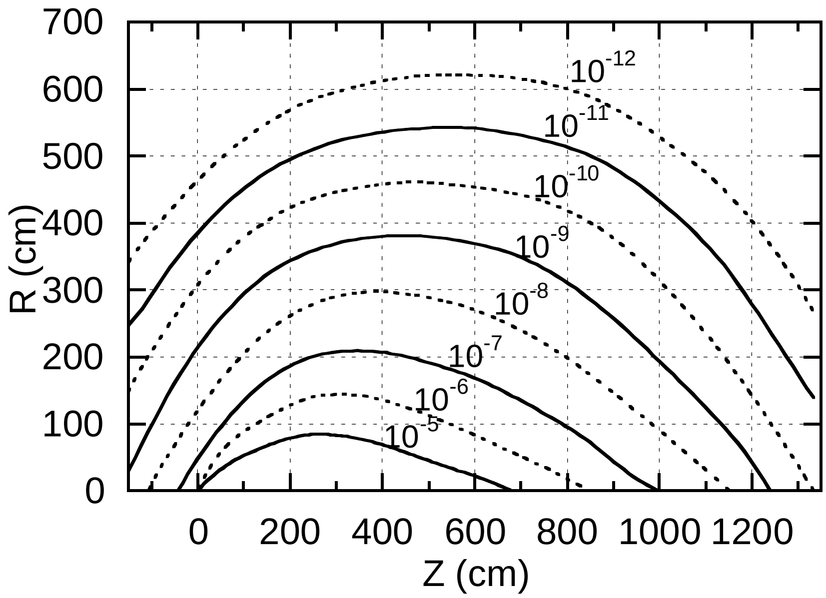


Fig. B1.c Monte Carlo results for 1 TeV/c protons incident on a CONCRETE cylinder. Contours of equal star density (stars $cm^{-3}$) per incident proton are plotted. The beam of 0.3 x 0.3 cm cross section is centered on the cylinder axis and starts to interact at zero depth. The star density includes only those due to hadrons above 0.3 GeV/c momentum. Contours of higher star density are not shown for clarity while those of lower star density are not included due to statistical uncertainty. [Adapted from (Va75).]

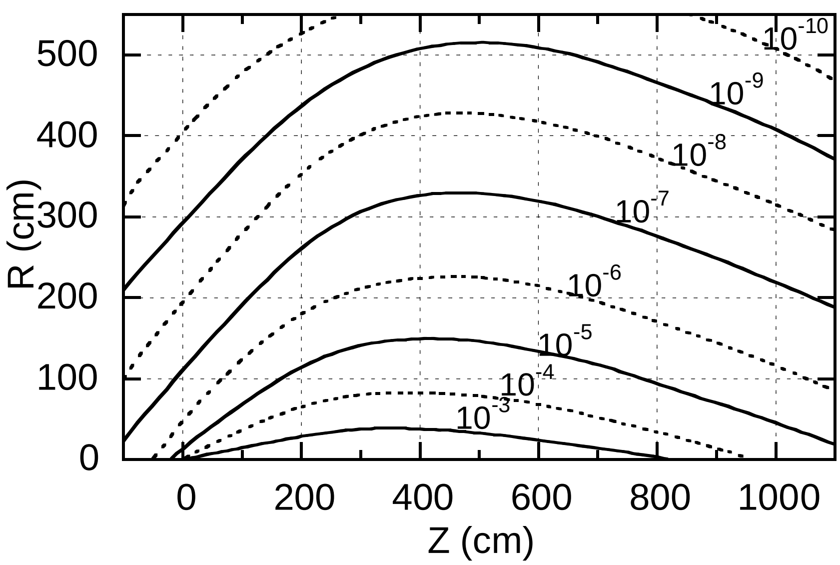


Fig. B1.d Monte Carlo results for 10 TeV/c protons incident on a CONCRETE cylinder. Contours of equal star density (stars $cm^{-3}$) per incident proton are plotted. The beam of 0.3 x 0.3 cm cross section is centered on the cylinder axis and starts to interact at zero depth. The star density includes only those due to hadrons above 0.3 GeV/c momentum. Contours of higher star density are not shown for clarity while those of lower star density are not included due to statistical uncertainty. [Adapted from (Va75).]

## B.2 Results for Solid IRON Cylinders

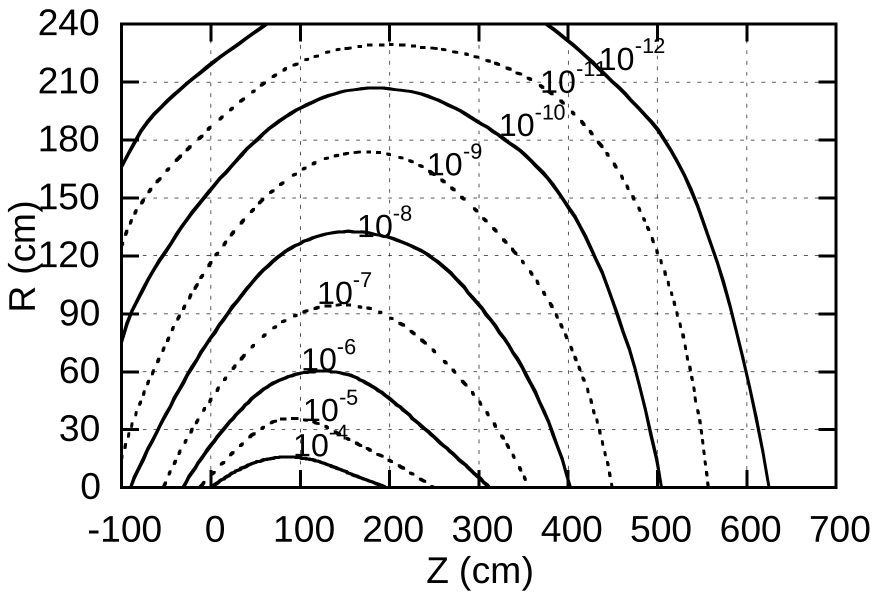


Fig. B2.a Monte Carlo results for 30 GeV/c protons incident on an IRON cylinder. Contours of equal star density (stars $cm^{-3}$) per incident proton are plotted. The beam of 0.3 x 0.3 cm cross section is centered on the cylinder axis and starts to interact at zero depth. The star density includes only those due to hadrons above 0.3 GeV/c momentum. Contours of higher star density are not shown for clarity while those of lower star density are not included due to statistical uncertainty. [Adapted from (Va75).]

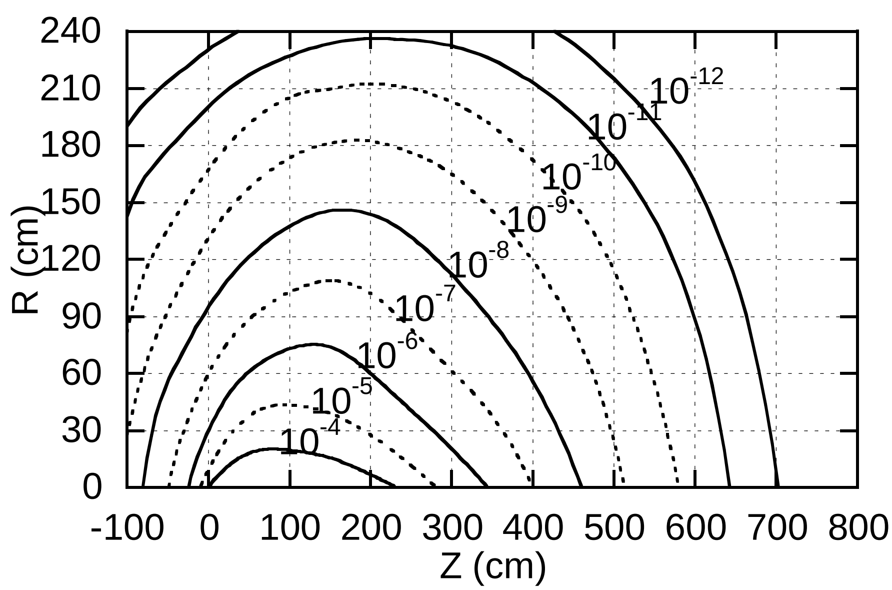


Fig. B2.b Monte Carlo results for 100 GeV/c protons incident on an IRON cylinder. Contours of equal star density (stars $cm^{-3}$) per incident proton are plotted. The beam of 0.3 x 0.3 cm cross section is centered on the cylinder axis and starts to interact at zero depth. The star density includes only those due to hadrons above 0.3 GeV/c momentum. Contours of higher star density are not shown for clarity while those of lower star density are not included due to statistical uncertainty. [Adapted from (Va75).]

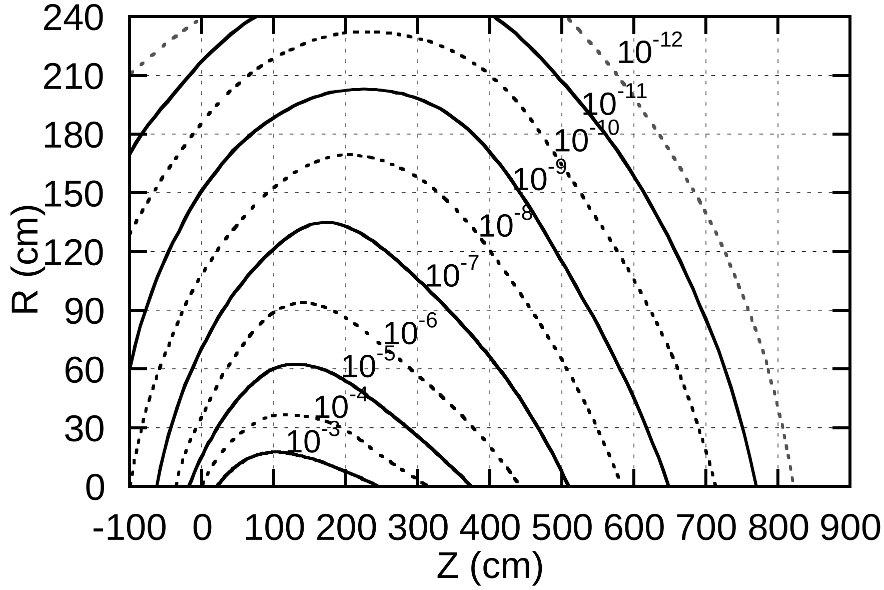


Fig. B2.c Monte Carlo results for 1 TeV/c protons incident on an IRON cylinder. Contours of equal star density (stars $cm^{-3}$) per incident proton are plotted. The beam of 0.3 x 0.3 cm cross section is centered on the cylinder axis and starts to interact at zero depth. The star density includes only those due to hadrons above 0.3 GeV/c momentum. Contours of higher star density are not shown for clarity while those of lower star density are not included due to statistical uncertainty. [Adapted from (Va75).]

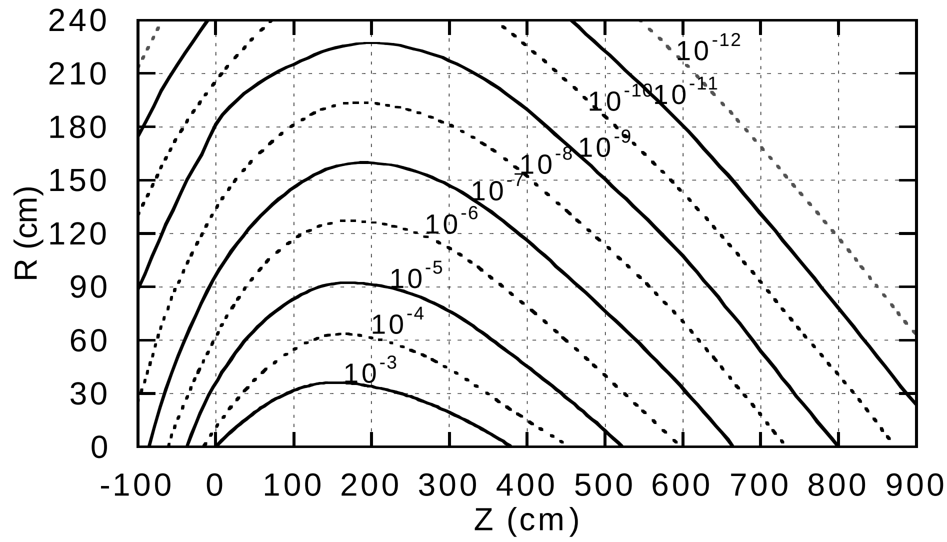


Fig. B2.d Monte Carlo results for 10 TeV/c protons incident on an IRON cylinder. Contours of equal star density (stars $cm^{-3}$) per incident proton are plotted. The beam of 0.3 x 0.3 cm cross section is centered on the cylinder axis and starts to interact at zero depth. The star density includes only those due to hadrons above 0.3 GeV/c momentum. Contours of higher star density are not shown for clarity while those of lower star density are not included due to statistical uncertainty. [Adapted from (Va75).]

## B.3 Results for 1 TeV Protons Incident on Pipes and Magnets

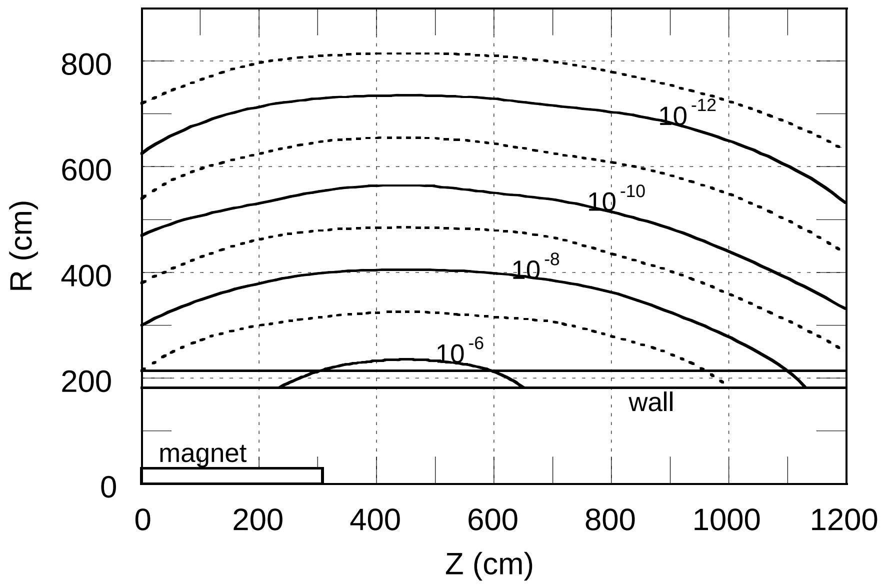


Fig. B3.a Contour plots of equal star density (stars cm$^{-3}$) per incident proton calculated using CASIM for a 1 TeV proton beam incident "head on" on the inner edge of one of the pole pieces one standard deviation of beam width deep. The magnet was rectangular with an aperture was 3.8 x 12.7 cm and outer dimensions of 31.8 x 40.6 cm. The results were averaged over azimuth and the magnet was centered in a cylindrical tunnel 182 cm in radius. The concrete wall was 30.48 cm thick and was surrounded by soil. [Adapted from Co82b.]

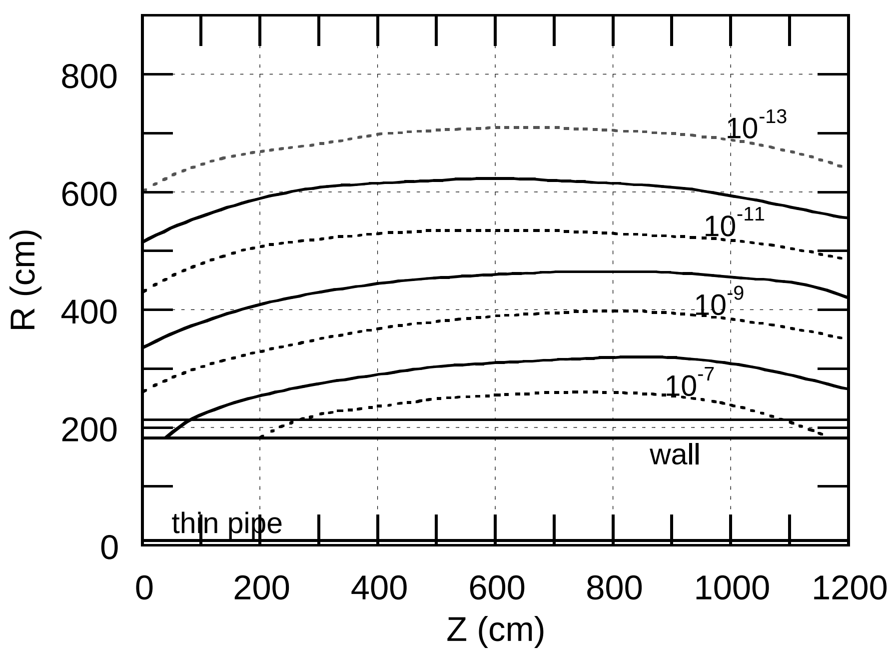


Fig. B3.b Contour plots of equal star density (stars cm$^{-3}$) per incident proton calculated using CASIM for a 1 TeV proton beam incident "head on" on a thin aluminum pipe of 10.16 cm outside diameter with 0.318 cm thick walls. The results were averaged over azimuth and the pipe was centered in a cylindrical tunnel 182 cm in radius. The concrete wall was 30.48 cm thick and was surrounded by soil. [Adapted from Co82b.]

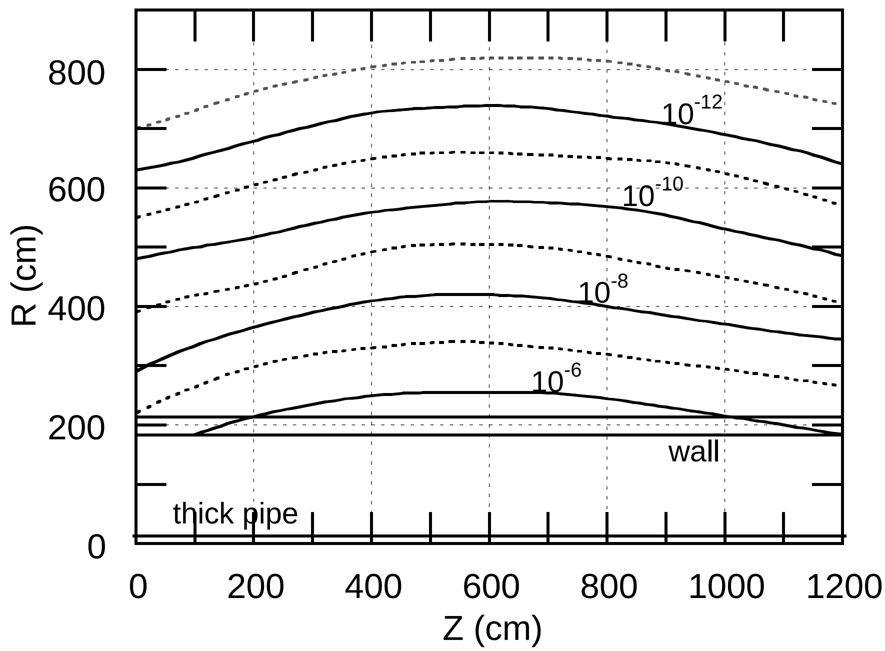


Fig. B3.c Contour plots of equal star density (stars cm$^{-3}$) per incident proton calculated using CASIM for a 1 TeV proton beam incident "head on" on a thick iron pipe of 30.48 cm outside diameter with1.27 cm thick walls. The results were averaged over azimuth and the pipe was centered in a cylindrical tunnel 182 cm in radius. The concrete wall was 30.48 cm thick and was surrounded by soil. [Adapted from Co82b.]

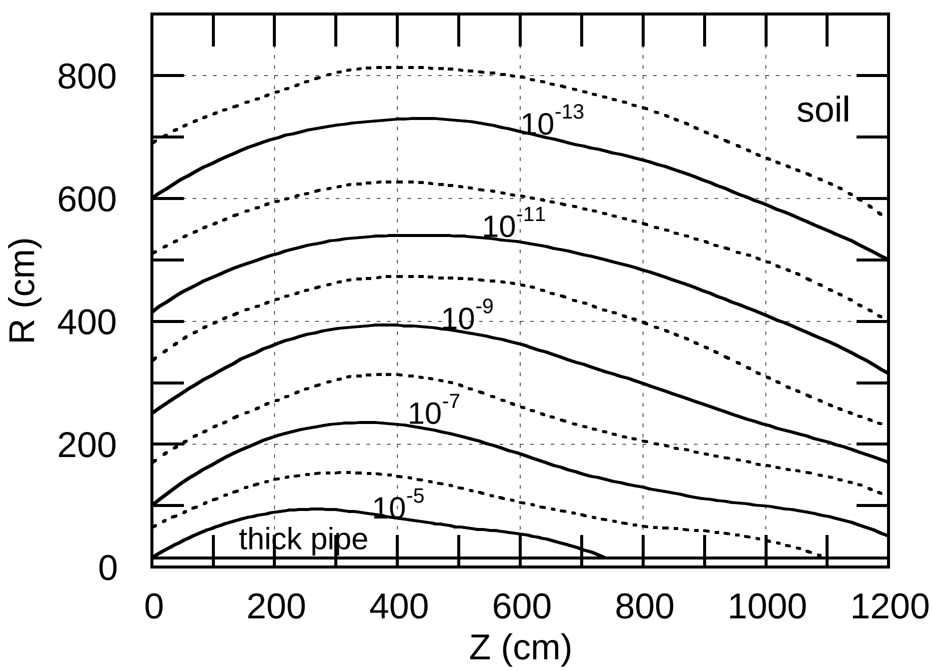


Fig. B3.d Contour plots of equal star density (stars cm$^{-3}$) per incident proton calculated using CASIM for a 1 TeV proton beam incident "head on" on a thick iron pipe of 30.48 cm outside diameter with 1.27 cm thick walls. The pipe is surrounded by soil. [Adapted from Co82b.]